The Tetratricopeptide Repeat Domain 7 Gene Is Mutated in Flaky Skin Mice: A Model for Psoriasis, Autoimmunity, and Anemia

CYNTHIA HELMS,* STEPHEN PELSUE,† LI CAO,* ERIKA LAMB,† BRETT LOFFREDO,† PATRICIA TAILLON-MILLER,* BROOKE HERRIN,* LISA M. BURZENSKI,§ BRUCE GOTT,§ BONNIE L. LYONS,§ DEANA KEPPLER,* LEONARD D. SHULTZ,§ AND ANNE M. BOWCOCK*,‡,[1]

*Department of Genetics, Washington University School of Medicine, St. Louis, Missouri 63110; †Department of Applied Medical Sciences, University of Southern Maine, Portland, Maine 04103; ‡Division of Dermatology, Department of Medicine, Washington University School of Medicine, St. Louis, Missouri 63110; and §The Jackson Laboratory, Bar Harbor, Maine 04609

The flaky skin *(fsn)* mutation in mice causes pleiotropic abnormalities including psoriasiform dermatitis, anemia, hyper-IgE, and anti-dsDNA autoantibodies resembling those detected in systemic lupus erythematosus. The *fsn* mutation was mapped to an interval of 3.9 kb on chromosome 17 between *D17Mit130* and *D17Mit162*. Resequencing of known and predicted exons and regulatory sequences from this region in *fsn/fsn* and wild-type mice indicated that the mutation is due to the insertion of an endogenous retrovirus (early transposon class) into intron 14 of the Tetratricopeptide repeat (TPR) domain 7 *(Ttc7)* gene. The insertion leads to reduced levels of wild-type *Ttc7* transcripts in *fsn* mice and the insertion of an additional exon derived from the retrovirus into the majority of *Ttc7* mRNAs. This disrupts one of the TPRs within TTC7 and may affect its interaction with an as-yet unidentified protein partner. The *Ttc7* is expressed in multiple types of tissue including skin, kidney, spleen, and thymus, but is most abundant in germinal center B cells and hematopoietic stem cells, suggesting an important role in the development of immune system cells. Its role in immunologic and hematologic disorders should be further investigated. Exp Biol Med 230:659–667, 2005

Key words: flaky skin mutation; *fsn*; *Ttc7* gene; psoriasis; autoimmunity; anemia

Introduction

The autosomal recessive mouse flaky skin *(fsn)* mutation arose spontaneously in A/J mice at The Jackson Laboratory (Bar Harbor, Maine), and we mapped it to distal mouse chromosome 17 (1). As we have previously reported, it is responsible for pleiotropic abnormalities in the skin, gastrointestinal tract, and immune and hematopoietic systems. Because the *fsn* mutation was extremely deleterious when maintained on the A/J strain background, we backcrossed it onto the BALB/cBy strain (1). Homozygous *fsn/fsn* mice appear normal at birth except for a hypochromic anemia but, subsequently, they develop a skin phenotype that is remarkably similar to human psoriasis: acanthosis with focal parakeratotic hyperkeratosis, subcorneal pustules, elongation of rete ridges, dermal capillary dilation, and marked diffuse dermal infiltrate of mixed inflammatory cells that are predominantly lymphocytes (2). A high density of collagen fibers and cellular infiltrates are seen in the papillary dermis, and numerous macrophages and mast cells lie at the dermal-epidermal junction in close proximity to focal dissolutions of the basement membrane. There is also intraepidermal invasion by neutrophils (3). We have previously reported that increased numbers of mast cells are observed in the skin and in the squamous epithelial portion of the stomach where papillomas are observed (4). Other pathologic changes that we have described in *fsn/fsn* mice include testicular degeneration, accumulation of inflammatory cells in the liver, and increased apoptosis of cecal enterocytes (5). The *fsn* mutation causes peripheral lymphadenopathy, CD4/CD8 imbalance, and hyperresponsiveness to T-cell growth factors (4, 6). Peripheral lymphocytes of *fsn/fsn* mice are also hyperactivated and hyperresponsive to IL-2, IL-4, and IL-7 (7, 8).

We observed that serum IgE levels are increased by ~7000-fold in *fsn/fsn* mice compared with normal littermates, and this increase is associated with elevated IL-4 production by splenocytes. Serum IgM, IgG1, and IgG2b

This work was supported in part by the National Institutes of Health Grants HL077642 and CA34196 (L.D.S.), AR4452904 (A.M.B., S.P., L.D.S.), and AR049049 (A.M.B.).

[1] To whom correspondence should be addressed at Department of Genetics, Washington University School of Medicine, 4566 Scott Avenue, St. Louis, MO 63110. E-mail: bowcock@genetics.wustl.edu

Received May 25, 2005.
Accepted June 23, 2005.

1535-3702/05/2309-0659$15.00

levels are also increased, while IgG3 is decreased. Elevated major histocompatibility complex (MHC) class II expression is also found in splenic B cells of *fsn/fsn* mice (4). There are also circulating anti-dsDNA autoantibodies accompanied by immune complex deposition in the kidneys, which result in glomerulonephritis (4, 9).

To elucidate the molecular basis of the *fsn* mutation, a positional cloning approach was carried out to identify the altered gene. This included refinement of the *fsn* map location by high-resolution genetic mapping, followed by resequencing of candidate genes within the interval. A comparison with A/J and BALB wild-type mice indicated that an endogenous retrovirus of the early transposon (ETn) class had been inserted into 57 base pairs 5′ to the splice-acceptor site of exon 15 of the Tetratricopeptide repeat (TPR) domain 7 (*Ttc7*) gene in *fsn/fsn* mice. This leads to the majority of *Ttc7* transcripts harboring a spliced exon of the ETn element and the addition of 61 amino acids into one of the TPRs, which is likely to abolish the function of this TPR-containing domain.

Materials and Methods

Mice. The following strains of mice were raised in our research colony at The Jackson Laboratory: BALB/cBy-*fsn/fsn* (CByJ.A-*fsn/fsn*), BALB/cByJ-*Prkdc*^{scid}/*Prkdc*^{scid} (CBy-*scid/scid*), CByJ.A-*fsn/fsn scid/scid*, CAST/EiJ, and DBA/2J.

Refinement of the fsn Interval. High-resolution genetic mapping was accomplished by the generation of two crosses, as previously described (1). An intersubspecific F2 analysis was accomplished by mating ovariectomized CBy-*scid/scid* females bearing CByJ.A-*fsn/fsn* ovaries with CAST/EiJ males. The F2 progeny of the (CByJ.A × CAST/EiJ)F1 +/*fsn* intercross were analyzed with simple sequence-length polymorphism primers (SSLP), as indicated in the text. Specific SSLP markers were chosen based on their localization within the previously identified fsn interval (10), as well as being polymorphic between BALB/cByJ and either CAST/Ei or DBA/2J. An additional F2 analysis was accomplished by mating ovariectomized CBy-*scid/scid* females bearing CByJ.A-*fsn/fsn* ovaries with DBA/2J males. The F2 progeny of the (CByJ.A × DBA/2J)F1 +/*fsn* intercross was analyzed with SSLP, as indicated in the text. The DNA samples were collected from tail biopsy tissue from snap-frozen kidney following sacrifice of the animal by CO_2 asphyxiation. The samples were prepared from tail biopsies by digesting tissue samples with proteinase K in PCR buffer nondetergent (PBND; 50 m*M* KCl, 10 m*M* Tris-HCl [pH 8.3], 2.5 m*M* $MgCl_2$, 0.1 mg/ml gelatin, 0.45% v/v Nonidet P40, and 0.45% v/v Tween 20) at 55°C overnight. A standard chloroform-phenol methodology was used to prepare the kidney DNA samples.

Genotyping of the *fsn* locus was determined either directly by observation of the *fsn* phenotype (i.e., striations in the abdomen fur, low hematocrit, distended abdomen, evident skin lesions) in the progeny of the F2 cross or by test mating. Phenotypically normal mice with recombinations within the *fsn* locus were mated with ovariectomized *scid/scid* mice bearing *fsn/fsn* ovaries. The progeny were phenotyped, as previously indicated, to determine the genotype of the unknown recombinant parent. Mating pairs that generated *fsn/fsn* progeny identified the recombinant parental genotype as +/*fsn*, whereas mating pairs that generated only phenotypically normal offspring identified the recombinant parent as +/+ at the *fsn* locus.

The SSLP primers listed in the text were either purchased from Invitrogen (Carlsbad, CA) or synthesized by Sigma-Genosys (Woodlands, TX) from sequences obtained from The Jackson Laboratory's Mouse Genome Informatics database (www.informatics.jax.org). Recombination events were analyzed by the Map Manager QTX computer program to determine linkage association and statistics (11).

DNA Resequencing. Sequencing was performed on polymerase chain reaction–amplified gene products with primers for known and predicted exons and regulatory sequences from the fsn interval. Methods have been described elsewhere (12). Comparisons of resulting sequence were made to wild-type Ttc7 cDNA sequence (GenBank Accession No. NM_028639) and genomic sequence from the National Center for Biotechnology Information genome build 34. GenBank Accession No. Y17106 was used in BLAST comparisons for the ETn insertion sequence.

Expression Analyses. Northern blotting, RNA preparation, and reverse transcriptase-polymerase chain reaction analyses on RNA from tissue of BALB/cBy-*fsn*, A/J +/+, and BALB/cBy mice were performed with routine methods. The murine multiple-tissue Northern was obtained from Clontech (Mountainview, CA). The Ttc7 probe was obtained by amplification of DNA from expressed sequence tag (EST) clone BC023773 with primers TTC7F (CCTGCATTGGCTAGAAGAG) and TTC7R (CCCTGCATTGCTAGAAGAG). Primers TTC7L2 (CCGATGATCCCCAAATTATC) and TTC7RE15 (ACTTGCTAGCGCTGCTCTTC) from exons 14 and 15, respectively, were used for amplification of wild-type and fsn transcripts from the kidney, skin, and thymus. These products were subjected to direct sequencing.

Human Association Studies. These analyses were performed with nine single-nucleotide polymorphisms (SNPs) lying within and flanking the human TTC7A gene. As previously described (12), 242 Caucasian nuclear families with psoriasis were included: 199 families with 2 affected children, 19 families with 1 affected child, 10 families with 3 affected children, 2 families with 4 affected children, 1 family with 6 affected children, and 1 family with 8 affected children. There were also a total of 142 trios in which both parents were available for genotyping. Collection of blood from family members was obtained with approval from institutional review boards overseen by the Washington University School of Medicine and Texas

Dermatology. The SNP genotyping and methods for family-based association analyses are described elsewhere (13).

Results

High-Resolution Genetic Mapping of the *fsn* Locus. Initial genetic mapping of the *fsn* locus linked the mutation to the genetic marker *D17Mit2* on distal mouse chromosome 17 (1). Subsequent mapping by intersubspecific F2 analysis localized the *fsn* locus to a region between *D17Mit75* and *D17Mit123* on distal mouse chromosome 17 (10). Based on this initial cross of 62 mice, the genetic distance was determined to be 4.1 cM. Two additional genetic crosses were undertaken to better define the location of the *fsn* locus: a (CByJ.A × CAST/Ei)F1 +/*fsn* intersubspecific (CAST-*fsn*) intercross and a (CByJ.A × DBA/2J)F1 +/*fsn* intercross (DBA-*fsn*). The CAST-*fsn* cross generated 593 F2 mice (1186 meiotic events), and the DBA-*fsn* cross generated 927 mice (1854 meiotic events). The CAST-*fsn* cross generated 62 recombinants between *D17Mit75* and *D17Mit123* and established a genetic distance of 5.23 cM for this region. The recombinants from the CAST-*fsn* cross were then further analyzed using nine additional SSLP markers and established a high-resolution genetic map of this region (Fig. 1).

Informative recombinants were mated with ovariectomized CBy/J-*scid/scid* mice bearing *fsn/fsn* ovaries, as indicated in the Materials and Methods section, to determine the location of the fsn locus relative to the markers on the genetic linkage map. The results of these analyses placed the *fsn* locus between *D17Mit130* and *D17Mit129* (Table 1).

The DBA/2J-*fsn* cross generated 31 recombinants between genetic markers *D17Mit41* and *D17Mit123*. This established a genetic distance of 3.9 cM between *D17Mit41* and *D17Mit123*. These recombinants were further analyzed with the markers *D17Mit130* and *D17Mit162* to generate the second high-resolution genetic linkage map, as depicted in Figure 1. An analysis of the CAST-*fsn* cross had determined that the *fsn* locus was tightly linked to *D17Mit130*. Therefore, we performed test matings of 31 informative recombinant mice (between *D17Mit41* and *D17Mit130*) to determine the location of the *fsn* locus on the DBA-*fsn* high-resolution genetic map. The *fsn* locus was determined to be located 0.5 cM distal to *D17Mit162* and 0.3 cM proximal to *D17Mit130* (Table 2). The location of the *fsn* locus, as well as the common markers *D17Mit123* and *D17Mit130*, were consistent between the two high-resolution maps and substantially reduced the region from the previous maps.

Gene Identification. As the mouse genomic sequence became available, we directed our efforts to genomic sequencing of all candidate genes/exons in the *fsn* interval identified by the genetic mapping. The candidate region extended from *D17Mit162* at chr17:82,191,243–82,391,359 to *D17Mit130* at chr17:85,893,389–86,093,618 (NCBI Build #33, University of California-Santa Cruz [UCSC], May 2004), a physical distance of 3.9 Mb. Genes in the interval included *Kcng3*, *Mta3*, *Zfp3612*, *BC052885*, *AK044550*, *Plekhh2*, *D2Lic*, *Abcg5*, *Abcg8*, *Lrpprc*, *ppm1b*, *Slc3a1*, *Flj23451*, *Six3*, *Six2*, *Flj10379*, *Prkce*, *Epas*, *Atp6*, *Viel2*, *TC10*, *Pigf*, *Cript*, *Socs5*, *Sdnsf*, *Ttc7*, and *Calm2*. Resequencing of known and predicted exons and regulatory sequences within this interval failed to identify any mutations that had arisen in *fsn* mice on the A/J background. However, we were not able to amplify exon 15 of *Ttc7* from *fsn/fsn* template DNA with primers flanking the exon, although A/J and BALB/cByJ wild-type DNA yielded the expected-sized products.

Long-range PCR amplification and resequencing of the resultant products from this region revealed a 5.542-kb insertion of an ETn element into intron 14 of *fsn/fsn* DNA, but not into A/J or BALB/cByJ wild-type DNA. This insertion was 57 base pairs 5′ to the splice acceptor of exon 15 of the *Ttc7* gene.

The ETn insertion had a 5490/5542 nucleotide (98%) identity to GenBank sequence Y17106. This was originally described as an ETn insertion mutation in a SELH/Bc mouse tyrosinase gene (14). The ETn family apparently originated as a recombination of MusD transposon with unrelated DNA and has long-terminal repeats (LTRs) similar to MusD elements, but does not include genes needed to transpose and; therefore, requires MusD provirus gene products for mobilization (15). The ETn found in the

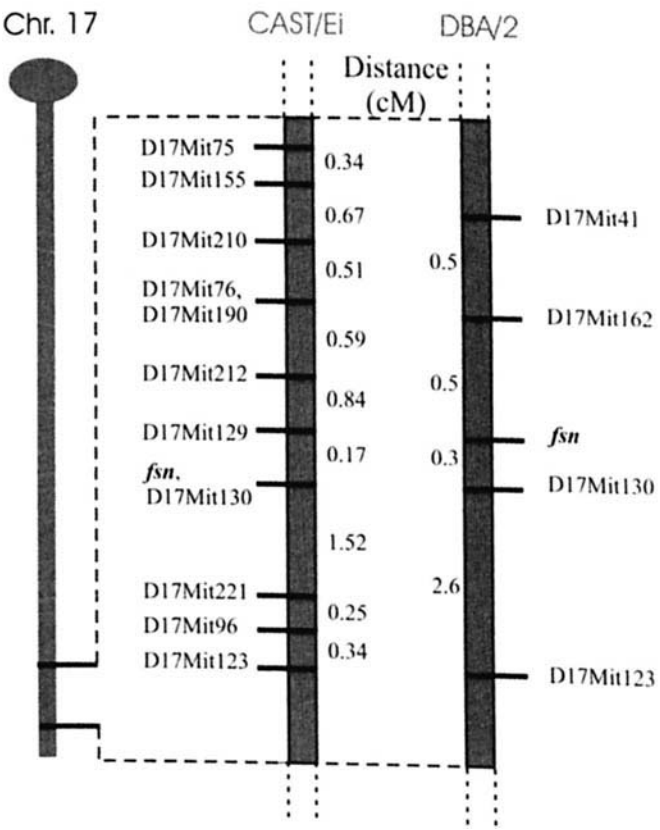

Figure 1. Refinement of the *fsn* interval. Two genetic crosses, CAST-*fsn* and DBA-*fsn*, were established to develop a high-resolution map of the *fsn* interval. In both crosses, the *fsn* locus was tightly linked to *D17Mit130*.

Table 1. Recombination Profile for (CBy.A/J × CAST/Ei)F1 +/*fsn* Intersubspecific Intercross Mice[a]

Marker interval	No. of recombinants	Distance (cm)	SE	LOD
D17Mit75–D17Mit155	4	0.34	0.17	173.0
D17Mit155–D17Mit210	8	0.67	0.24	168.4
D17Mit210–D17Mit76	6	0.51	0.21	170.6
D17Mit76–D17Mit190	0	0.00	0.00	178.8
D17Mit190–D17Mit212	7	0.59	0.22	168.4
D17Mit212–D17Mit129	10	0.84	0.27	166.3
D17Mit129–*fsn*	2	0.17	0.12	174.7
fsn–D17Mit130	0	0.00	0.00	177.9
D17Mit130–D17Mit221	18	1.52	0.36	158.3
D17Mit221–D17Mit96	3	0.25	0.15	173.0
D17Mit96–D17Mit123	4	0.34	0.17	173.0
Total	62	5.23	—	—

[a] $N = 593$.

fsn mouse insertion has an LTR nearly identical to the Y17106 LTR sequence. At the point of ETn insertion, the sequence CCATTC has been duplicated. This is consistent with previous reports of transposable element integration, which leads to the duplication of an odd number of base pairs (usually 5 or 7) at the integration site and flanking the mobile element.

Organization of the *Ttc7* Gene in Mice and the Orthologous *Ttc7* Gene in Humans. The organization of the human and mouse genes is very similar. Both have 20 exons, and both harbor a total of 7 TPRs in 2 regions that lie within exons 12–15 and exons 18–20 (Fig. 2). Table 3 shows the alignment of the different TPRs of this gene from human and mouse. The translated protein with the disrupted TPR-D lacks any PfamA-recognized repeat between TPR-C and TPR-E, indicating that the 3-unit, TPR-containing domain is abolished. Therefore, the ETn insertion would lead to a mutated TTC7 protein where one of the TPRs was disrupted by the insertion of a 61 amino acid peptide (Table 3 footnote). This may abolish interaction with an important protein partner.

Gene Expression in Normal and Mutant Mice. Northern blotting indicated that *Ttc7* is expressed as an ~4.8 kb transcript in normal mice, with high levels of expression in the liver, kidney, spleen, lower skin levels (not shown), heart (where at least two major transcripts were detected), and lung (Fig. 3a). The RT-PCR analyses also confirmed expression in the thymus, stomach, and lung in wild-type mice (not shown).

Next, we determined if this insertion in *fsn/fsn* mice altered levels or size of *Ttc7* transcripts. Northern blotting indicated that *Ttc7* is expressed at reduced levels in the kidney, as well as in the liver, skin, and spleen (not shown) of CByJ.A-*fsn/fsn* vs. A/J or BALB/cByJ wild-type mice (Fig. 3b), although the transcript size was similar.

The RT-PCR, with primers from exons 14–15 flanking the ETn insertion, generated the expected-sized product of 143bp in A/J and BALB/cByJ wild-type mice. However, amplification of cDNAs from the thymus and kidney generated a major 325bp product from CByJ.A-*fsn/fsn* mice (Fig. 3c). Resequencing of this product indicated that it was derived from the splicing of the ETn sequence from bp 246–428 of Y17106. Lower levels of correctly spliced wt *Ttc7* were also detected in *fsn/fsn* cDNA, in addition to the mutant splice products.

The current repository of gene expression datasets allows one to perform expression analyses *in silico*. We used the SOURCE, web-based bioinformatics resource (16) to determine the expression profile of *Ttc7* based on EST datasets. Table 4 presents the relative percentage of *Ttc7* transcripts from different types of tissue. Lymphoid cells and tissue were among the top 15 highest-relative expression sources. Of particular note is the finding that B lymphocytes and hematopoietic stem cells are two of the top-ranked sources of *Ttc7* expression.

Table 2. Recombination Profile for (CBy.A/J × DBA/2J)F1 +/*fsn* Interspecific Intercross Mice[a]

Marker interval	No. of recombinants	Distance (cm)	SE	LOD
D17Mit41–D17Mit162	6	0.5	0.2	279.3
D17Mit162–*fsn*	7	0.5	0.2	275.2
fsn–D17Mit130	5	0.3	0.1	341.4
D17Mit130–D17Mit123	13	2.6	0.7	89.5
Total	31	3.9	—	—

[a] $N = 927$.

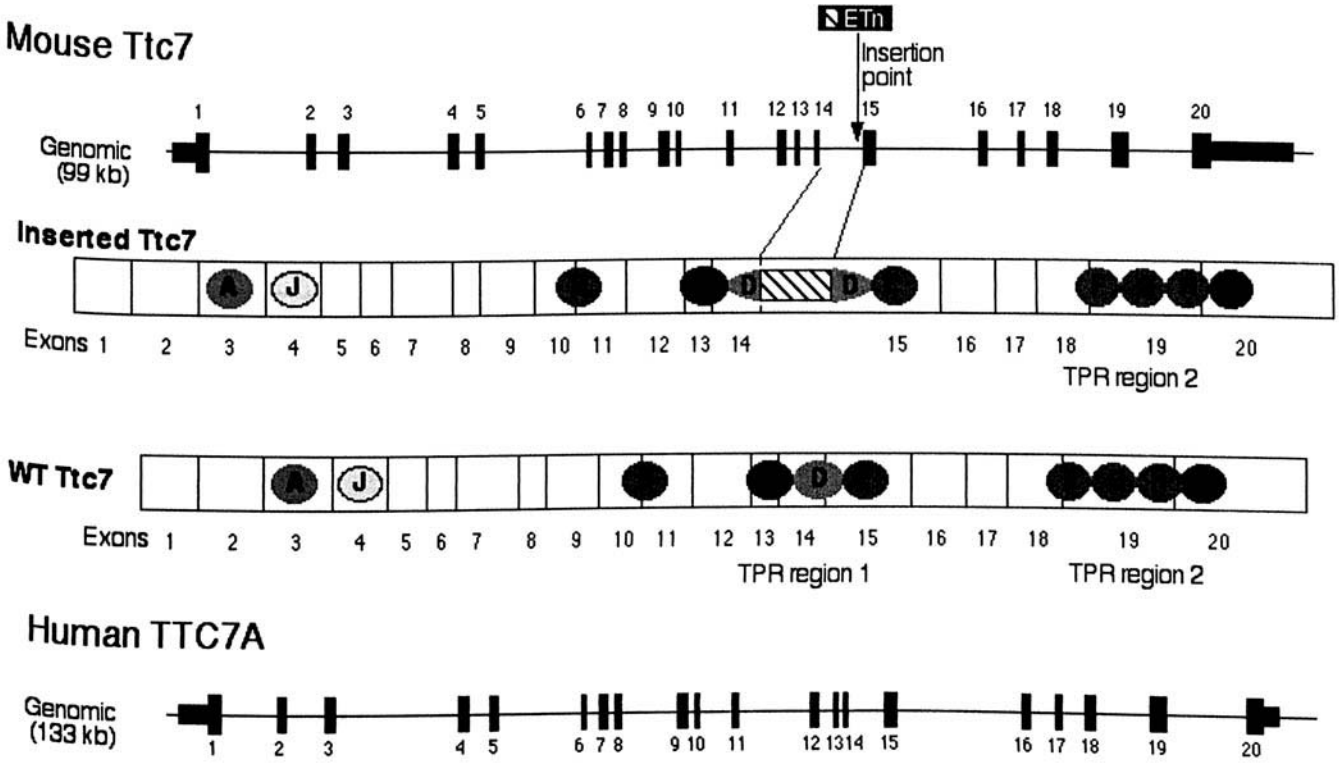

Figure 2. Comparison of genomic structure of human and mouse *TTC7A* genes. Both mouse *Ttc7* and human *TTC7A* genes from reference sequences have 20 exons with conserved exon sizes, except for 5′ and 3′ untranslated regions (UTRs). The TPRs in both genes have identical arrangements as determined from Pfam database results (36). The TPRs are shown as colored ovals on exons. The TPR-1 repeats are shown in purple (C, I). The TPR-2 repeats are green (B, E, F, G, H), and TPR-2 repeats determined from sequence context are blue (A, D). Repeats B, C, D, F, and H are formed by splice events. One repeat (J) is in the NCBI human annotation (accession = Q9ULT0), but not in the mouse annotation (accession = Q8BGB2). Human isoform 2 does not have TPR-A. The TPR repeats from regions 1 and 2 are likely to be the only interactive units, as three repeats are the minimally functional unit (37). The figure is approximate, not to scale.

Lymphocyte Contribution to the *fsn* Phenotype. The expression profile indicates that *Ttc7* is expressed in lymphoid tissues. Lymphocyte defects have been associated with the development of systemic autoimmunity in *fsn/fsn* mice. We sought to determine if lymphocytes significantly contributed to the *fsn* phenotype by determining the effect of the severe combined immunodeficiency $Prkdc^{scid}$ *(scid)* mutation. Previous analysis of the lymphocyte-deficient, double-mutant CByJ.A-*fsn/fsn scid/scid* mice indicated that this strain maintained skin lesions and anemia (17). Further analysis determined that the T- and B-cell–deficient *fsn/fsn scid/scid* mice have substantially increased life spans compared with lymphocyte-sufficient *fsn/fsn* mice. The mean life span of the double mutant *fsn/fsn scid/scid* mice was not significantly different from that of the *+/fsn scid/scid* controls (261 ± 27 days vs. 314 ± 32 days; $P = 0.24$).

Linkage and Association With Psoriasis. Linkage analysis yielded a multipoint, nonparametric logarithm of the odds (LOD) score of 0.93 ($P = 0.16$), which is not significant, but also cannot rule-out the presence of a psoriasis locus at this site. Family-based association analyses were then performed with nine SNPs from within or flanking the human *TTC7A* gene and 242 nuclear families with psoriasis. The TDT-AE (transmission disequilibrium test-allowing for errors; Ref. 18) and the PDT (pedigree disequilibrium test; Ref. 19) were performed, and results of the PDT are provided in Table 5 (both were similar). When results were adjusted for multiple testing, none was significant. However, an examination of haplotypes yielded $P < 0.05$ for a three-marker haplotype defined by rs1433773, rs7558171, and rs6544950. This finding needs to be followed up with additional samples and markers from the region.

Discussion

The *Ttc7* is a novel gene of unknown function that encodes the TPR domain 7 protein. The TPRs typically contain 34 amino acids and are frequently found in multiprotein complexes in proteins from a variety of organisms, from bacteria to humans (20). They are reported to be involved in protein-protein interactions involving chaperones, the cell cycle, transcription, and protein transport (21, 22). The number of TPR motifs varies among proteins. In yeast, several members of the TPR family are genetically associated with proteins harboring WD-40 repeats, and it has been proposed that proteins containing the WD-40 repeat interact physically with members of the TPR-family *via* their respective repeated motifs (23).

The *fsn* mutation is due to the insertion of an ETn

Table 3. Alignment of Tetratricopeptide Repeats from Human and Mouse TTC7 Predicted Peptides

Repeat	Sp.	Position		Sequence
TPR A	Hs	121	157	CEAMLILGKLHYVEGSYRDAISMYARAGIDDMSMENK
	Mm	122	158	CEAMLILGKLHYVEGSYRDAVSMYARAGIDDISVENK
TPR J	Hs	177	210	ERLPNSIASRFRLTEREEEVITCFERASWIAQVF
	Mm	177	210	ERLPNSVASHIRLTEREEEVVACFERASWVAQVF
TPR B	Hs	414	447	FHLWYQVALSMVACGKSAYAVSLLRECVKLRPSD
	Mm	415	448	FHLWYQVALSMVACGKSAYAVSLLRECMKLQPSD
TPR C	Hs	497	531	YSLQATDATLKSKQDELHRKALQTLERAQQLAPSD
	Mm	498	532	YSLQATDATLKSKQDELHRKALQTLERARELAPDD
TPR D	Hs	532	565	PQVILYVSLQLALVRQISSAMEQLQEALKVRKDD
	Mm	533	566	PQIIFYVALQLALVRQISSAMERLQEALTMCRDD
TPR E	Hs	566	599	AHALHLLALLFSAQKHHQHALDVVNMAITEHPEN
	Mm	567	600	ANALHLLALLFSAQKYYQHALDVINMAITEHPEN
TPR F	Hs	711	744	EQIWLQAAELFMEQQHLKEAGFCIQEAAGLFPTS
	Ms	711	744	EQIWLQAAELFMEQRQLKEAGFCIQEAAGLFPTS
TPR G	Hs	745	778	HSVLYMRGRLAEVKGNLEEAKQLYKEALTVNPDG
	Mm	745	778	HSVLYMRGRLAEVKGSFEEAKQLYKEALTVNPDG
TPR H	Hs	779	812	VRIMHSLGLMLSRLGHKSLAQKVLRDAVERQSTC
	Mm	779	812	VRIMHSLGLMLSQLGHKSLAQKVLRDAVERQSTF
TPR I	Hs	813	846	HEAWQGLGEVLQAQGQNEAAVDCFLTALELEASS
	Mm	813	846	HEAWQGLGEVLQDQGQNEAAVDCFLTALELEASS

Peptide TPRs [36] from mouse Ttc7 (Q8BGB2) and human TTC7A (Q9ULT0) identified with Pfam [37] are colored as in Figure 2. TPRs belonging to potentially functional domains are boxed. The insertion results in a 61-aa (highlighted in yellow) disruption of TPR-D into:

PQIIFYVALQLALVRQI[PLLQLERPSQSNRSRCELLAAATFWRQNWDLKNGREM LRGTLHWSSTGKDLRIGHRSNGQI]SSAMERLQEALTMCRDD.

transposon into intron 14 of the *Ttc7* gene. This disrupts one of the TPRs and potentially abolishes interaction with one of its partners. This, or nearly complete loss of TTC7 function, could lead to the multiple pathologic changes seen in *fsn/fsn* mice. The *fsn* mutation results in abnormalities in multiple cell lineages including erythroid cells, lymphocytes, eosinophils, mast cells, and keratinocytes, as well as testicular degeneration and marked gastric changes (1–9). Thus, the wild-type *Ttc7* gene is likely to play an important role in multiple hematologic, immunologic, and other processes.

The ETn elements are among the most active murine mobile sequences. They are moderately repetitive sequences that are present in hundreds of copies in the mouse genome. Their length ranges from 4.4 kb to 7.1 kb, they contain LTRs on both sides, and they are flanked by target-site duplications (24). In recent years, several germ-line and somatic mutations caused by fresh ETn integrations have been found (24). These include a mutation that is responsible for the muted *(mu)* mouse (25), the *wiz* gene (24), and the Lep^{ob} mutation of obese mice (26). Another example of ETn integration resulting in autoimmunity caused by the $Tnfrsf6^{Lpr}$ (lymphoproliferation) mutation is a recessive trait due to a mutation in the *Tnfrsf6* gene (commonly referred to as *Fas*), which leads to a substantial reduction in *Tnfrsf6* transcript. One of the *Fas* mutations is due to an ETn insertion of DNA within the second intron of the *Tnfrsf6* gene (27–30). The defect is proposed to be leaky due to the production of intact *Tnfrsf6* mRNA as a result of the splicing out of the ETn that contains intron from primary *Tnfrsf6* transcripts. We observed a similar event in the case of *Ttc7* transcripts of *fsn/fsn* mice where the majority of transcripts are mutant, but where a small proportion of *Ttc7* transcripts are wild type.

Recently, a second mutant allele of *fsn* was identified in the hereditary erythroblastic anemia *(hea)* mouse. This mutation leads to a life span of only 1 week, severe skin lesions, and the reduction in red blood cell numbers, hematocrit, and hemoglobin (31). Homozygous *hea* mice also have elevated Zn protoporphyrin and serum iron. Aspects of the *hea* anemia can be transferred by hematopoietic stem-cell transplantation, and neonatal *hea/hea* mice show a similar hematologic phenotype to the *fsn* mutant. Both tissue-iron overloading and elevated serum iron are also found in *hea/hea* and *fsn/fsn* neonates. There is a shift from iron-overloading to iron-deficiency as the *fsn/fsn* mice age. The *fsn* anemia is cured by an iron-supplemented diet, which suggests an iron-utilization defect. Therefore, it was proposed that the gene mutated in *fsn/fsn* mice is also required for iron uptake into erythropoietic cells and for kidney iron resorption (31). Independently, this group recently proposed that the defect in these mice lies within the *Ttc7* gene (32). Moreover, deletion of this gene is responsible for the *hea* phenotype.

Our independent finding, based on thorough resequencing of the *fsn* candidate interval, confirms that *Ttc7* is indeed mutated in *fsn/fsn* mice and indicates that the altered protein harbors a disrupted TPR that may abolish interaction with an as-yet unidentified protein. In contrast to the study by White *et al.* (32), we also demonstrate that a subset of *Ttc7* transcripts of *fsn/fsn* mice are wild type, indicating that the splicing in of the ETn "exon" is leaky. Although White *et al.* (32) propose that the altered TTC7 protein affects iron transport, our observation is that *Ttc7* is highly expressed in both hematopoietic stem cells and germinal center B cells and; therefore, it may play a fundamental role in the development or regulation of the immune system. This is in agreement with the multiple immunologic abnormalities in *fsn/fsn* mice. Lymphoid abnormalities in *fsn/fsn* mice include B- and T-cell hyperactivation, accompanied by autoimmunity (4, 6–9). The role of autoreactive lymphocytes, in the pathologic changes observed in *fsn/fsn* mice is evidenced by our finding that lymphocyte-deficient *fsn/fsn scid/scid* mice have markedly increased life spans compared with *fsn/fsn* mice.

The complete deletion of the *Ttc7* gene in *Hea/Hea* mutant mice results in severe anemia accompanied by skin abnormalities (32). In contrast, the *fsn* mutation results in the presence of low levels of wild-type transcript, in addition to mutant splice products. The WBB6F1-*Hea/Hea* mice survive to only 1 week (32), while CBy.A-*fsn/fsn* mice live for 2 to 3 months. The increased life span of CBy.A-*fsn/fsn* mice compared with WBB6F1-*Hea/Hea* mice may be associated with the presence of some normal Ttc7 protein in *fsn/fsn* mice. However, the severity of the phenotype of *fsn/*

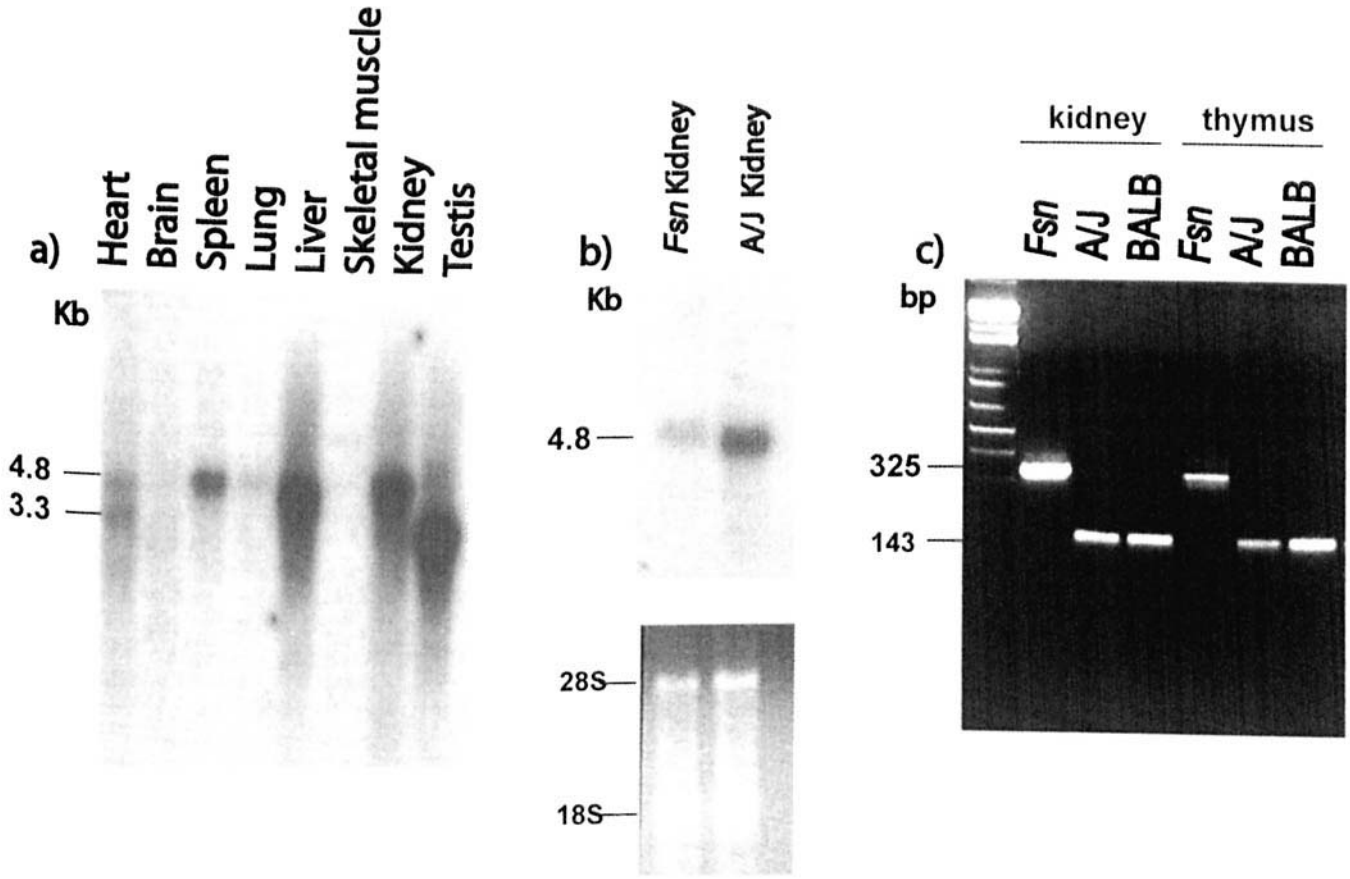

Figure 3. Expression of *Ttc7* in *fsn* and wild-type mice. (a) Multiple tissue Northern analysis with tissue from wild-type mice. (b) Upper panel: Northern analysis of RNA from A/J-*fsn/fsn* and wild-type A/J kidney. Lower panel: Original agarose gel showing equal loading of *fsn* and A/J RNA and the location of 28S and 18S RNAs. (c) Agarose gel analysis of RT-PCR of cDNA products from C.ByJ.A-*fsn/fsn*, wild-type A/J, and C.ByJ.A wild-type mice with exon 14 and 15 primers flanking the intron that harbors the ETn insertion.

Table 4. Abundance of *Ttc7* Transcripts in Embryonic and Adult Tissues[a]

Rank	Tissue	Normalized expression (%)
1	Germinal center B cell (resting spleen)	21.17
2	Submandibular gland	19.61
3	Hematopoietic stem cell (Lin–, c-Kit+, Sca-1–)	6.29
4	Vagina	4.42
5	13.5 post coitum whole embryo	4.21
6	Carcinoma	4.10
7	Spleen	3.07
8	Liver tumor	2.87
9	Colon	2.69
10	Kidney	2.64
11	Embryonic limb, maxilla, and mandible	2.43
12	Infiltrating ductal carcinoma	2.39
13	Bone	2.27
14	Thymus	2.15
15	Thymic tumor	2.12

[a] Expression is presented as normalized abundance, calculated by the number of unique *Ttc7* ESTs compared with the total number of ESTs in a given tissue.

Table 5. Results of Analyses Investigating the Association of *TTC7A* with Psoriasis

SNP	Position (UCSC, May 2004)	Allele	No. of trios	No. of transmitted chromosomes	No. of nontransmitted chromosomes	×2	PDT *P* value[a]
rs11690921	47065413	1	120	100	77	4.521	0.0335
rs11690921	47065413	2	120	140	163	—	—
rs1433773	47125581	1	129	167	167	0	1
rs1433773	47125581	2	129	91	91	—	—
rs7558171	47135406	1	129	92	94	0.028	0.8667
rs7558171	47135406	2	129	166	164	—	—
rs6544950	47135740	1	98	165	151	2.45	0.1175
rs6544950	47135740	2	98	31	45	—	—
rs17481349	47136837	1	65	121	114	2.333	0.1266
rs17481349	47136837	2	65	9	16	—	—
rs736377	47137542	1	154	72	89	2.513	0.1129
rs736377	47137542	2	154	236	219	—	—
rs6761800	47139808	1	117	66	81	1.957	0.1619
rs6761800	47139808	2	117	168	153	—	—
rs7570810	47149318	1	121	40	33	0.71	0.3994
rs7570810	47149318	2	121	202	209	—	—
rs1046263	47213395	1	49	76	82	1.5	0.2207
rs1046263	47213395	2	49	22	16	—	—

[a] Results obtained with the TDT-AE (18) using only trios were very similar to those presented here.

fsn mutant mice is modified by the background strain (1), and it is possible that differences in phenotype between *fsn/fsn* and *Hea/Hea* mutant mice are due, in part, to effects of background-modifying genes. Future functional analyses of the encoded protein may provide insight into the development of anemia and psoriasis in humans.

Gaining an understanding of the molecular defects that result in human psoriasis is difficult due to the heterogeneity of the disease, the variable contribution of the environment, and the variable mode of inheritance. The identification of a gene predisposing a similar phenotype in mouse, followed by the isolation of the corresponding human ortholog, has facilitated investigations of mechanisms underlying a number of autoimmune diseases. A number of mouse mutations have been described that alter hematopoiesis, some of which lead to autoimmunity and/or skin defects (33–35). Histologically, the skin of the *fsn/fsn* mouse is very similar to that seen in psoriatic lesional skin. Our preliminary investigation of the association of SNPs within *TTC7A*, the human ortholog of mouse *Ttc7* with psoriasis susceptibility, did not reveal a major role for this locus in this disease. However, an investigation of how the *Ttc7 fsn* mutation leads to an inflammatory skin disorder should be investigated. Moreover, the role of this gene in other immunologic disorders and autoimmune diseases, such as systemic lupus erythematosus, should be studied given the observation that *fsn/fsn* mice harbor circulating anti-dsDNA autoantibodies and exhibit additional aspects of autoimmune disease (9).

We thank Ken Johnson, Greg Cox, Jennifer Gardner, and Michael Lovett for their critical reviews of the manuscript and Christina Zhao, Fenghe Du, Rebecca Wolfe, Jil Daw, Rebecca Cochran, Vaisu Patel, Raymond Miller, Shenghui Duan, Pam Lang, and Allison Ingalls for their technical help.

1. Beamer WG, Pelsue SC, Shultz LD, Sundberg JP, Barker JE. The flaky skin (fsn) mutation in mice: map location and description of the anemia. Blood 86:3220–3226, 1995.
2. Sundberg JP, Dunstan RW, Roop DR, Beamer WG. Full-thickness skin grafts from flaky skin mice to nude mice: maintenance of the psoriasiform phenotype. J Invest Dermatol 102:781–788, 1994.
3. Morita K, Hogan ME, Nanney LB, King LE Jr, Manabe M, Sun TT, Sundberg JP. Cutaneous ultrastructural features of the flaky skin (fsn) mouse mutation. J Dermatol 22:385–395, 1995.
4. Pelsue SC, Schweitzer PA, Schweitzer IB, Christianson SW, Gott B, Sundberg JP, Beamer WG, Shultz LD. Lymphadenopathy, elevated serum IgE levels, autoimmunity, and mast cell accumulation in flaky skin mutant mice. Eur J Immunol 28:1379–1388, 1998.
5. Sundberg JP, France M, Boggess D, Sundberg BA, Jenson AB, Beamer WG, Shultz LD. Development and progression of psoriasiform dermatitis and systemic lesions in the flaky skin (fsn) mouse mutant. Pathobiology 65:271–286, 1997.
6. Abernethy NJ, Hagan C, Tan PL, Birchall NM, Watson JD. The

peripheral lymphoid compartment is disrupted in flaky skin mice. Immunol Cell Biol 78:5–12, 2000.
7. Abernethy NJ, Hagan C, Tan PL, Watson JD. Dysregulated expression of CD69 and IL-2 receptor alpha and beta chains on CD8+ T lymphocytes in flaky skin mice. Immunol Cell Biol 78:596–602, 2000.
8. Welner R, Hastings W, Hill BL, Pelsue SC. Hyperactivation and proliferation of lymphocytes from the spleens of flaky skin (fsn) mutant mice. Autoimmunity 37:227–235, 2004.
9. Withington S, Maltby-Askari E, Welner R, Parker R, Pelsue SC. Antinuclear autoantibodies in flaky skin (fsn) mutant mice. Autoimmunity 35:175–181, 2002.
10. Pelsue SC, Schweitzer PA, Beamer WG, Shultz LD. Mapping of the flaky skin (fsn) mutation on distal mouse chromosome 17. Mamm Genome 6:758, 1995.
11. Manly KF, Cudmore RH Jr, Meer JM. Map Manager QTX: cross-platform software for genetic mapping. Mamm Genome 12:930–932, 2001.
12. Speckman RA, Wright Daw JA, Helms C, Duan S, Cao L, Taillon-Miller P, Kwok PY, Menter A, Bowcock AM. Novel immunoglobulin superfamily gene cluster, mapping to a region of human chromosome 17q25, linked to psoriasis susceptibility. Hum Genet 112:34–41, 2003.
13. Helms C, Cao L, Krueger JG, Wijsman EM, Chamian F, Gordon D, Heffernan M, Daw JA, Robarge J, Ott J, Kwok PY, Menter A, Bowcock AM. A putative RUNX1 binding site variant between SLC9A3R1 and NAT9 is associated with susceptibility to psoriasis. Nat Genet 35:349–356, 2003.
14. Hofmann M, Harris M, Juriloff D, Boehm T. Spontaneous mutations in SELH/Bc mice due to insertions of early transposons: molecular characterization of null alleles at the nude and albino loci. Genomics 52:107–109, 1998.
15. Mager DL, Freeman JD. Novel mouse type D endogenous proviruses and ETn elements share long terminal repeat and internal sequences. J Virol 74:7221–7229, 2000.
16. Diehn M, Sherlock G, Binkley G, Jin H, Matese JC, Hernandez-Boussard T, Rees CA, Cherry JM, Botstein D, Brown PO, Alizadeh AA. SOURCE: a unified genomic resource of functional annotations, ontologies, and gene expression data. Nucleic Acids Res 31:219–223, 2003.
17. Sundberg JP, Boggess D, Sundberg BA, Beamer WG, Shultz LD. Epidermal dendritic cell populations in the flaky skin mutant mouse. Immunol Invest 22:389–401, 1993.
18. Gordon D, Heath SC, Liu X, Ott J. A transmission/disequilibrium test that allows for genotyping errors in the analysis of single-nucleotide polymorphism data. Am J Hum Genet 69:371–380, 2001.
19. Martin ER, Bass MP, Kaplan NL. Correcting for a potential bias in the pedigree disequilibrium test. Am J Hum Genet 68:1065–1068, 2001.
20. Blom E, van de Vrugt HJ, de Vries Y, de Winter JP, Arwert F, Joenje H. Multiple TPR motifs characterize the Fanconi anemia FANCG protein. DNA Repair (Amst) 3:77–84, 2004.
21. Smith DF. Tetratricopeptide repeat cochaperones in steroid receptor complexes. Cell Stress Chaperones 9:109–121, 2004.
22. Blatch GL, Lassle M. The tetratricopeptide repeat: a structural motif mediating protein-protein interactions. Bioessays 21:932–939, 1999.
23. van der Voorn L, Ploegh HL. The WD-40 repeat. FEBS Lett 307:131–134, 1992.
24. Baust C, Baillie GJ, Mager DL. Insertional polymorphisms of ETn retrotransposons include a disruption of the wiz gene in C57BL/6 mice. Mamm Genome 13:423–428, 2002.
25. Zhang Q, Li W, Novak EK, Karim A, Mishra VS, Kingsmore SF, Roe BA, Suzuki T, Swank RT. The gene for the muted (mu) mouse, a model for Hermansky-Pudlak syndrome, defines a novel protein which regulates vesicle trafficking. Hum Mol Genet 11:697–706, 2002.
26. Moon BC, Friedman JM. The molecular basis of the obese mutation in ob2J mice. Genomics 42:152–156, 1997.
27. Kobayashi S, Hirano T, Kakinuma M, Uede T. Transcriptional repression and differential splicing of Fas mRNA by early transposon (ETn) insertion in autoimmune lpr mice. Biochem Biophys Res Commun 191:617–624, 1993.
28. Adachi M, Watanabe-Fukunaga R, Nagata S. Aberrant transcription caused by the insertion of an early transposable element in an intron of the Fas antigen gene of lpr mice. Proc Natl Acad Sci U S A 90:1756–1760, 1993.
29. Wu J, Zhou T, He J, Mountz JD. Autoimmune disease in mice due to integration of an endogenous retrovirus in an apoptosis gene. J Exp Med 178:461–468, 1993.
30. Chu JL, Drappa J, Parnassa A, Elkon KB. The defect in Fas mRNA expression in MRL/lpr mice is associated with insertion of the retrotransposon, ETn. J Exp Med 178:723–730, 1993.
31. White RA, McNulty SG, Roman S, Garg U, Wirtz E, Kohlbrecher D, Nsumu NN, Pinson D, Gaedigk R, Blackmore K, Copple A, Rasul S, Watanabe M, Shimizu K. Chromosomal localization, hematologic characterization, and iron metabolism of the hereditary erythroblastic anemia (hea) mutant mouse. Blood 104:1511–1518, 2004.
32. White RA, McNulty SG, Nsumu NN, Boydston LA, Brewer BP, Shimizu K. Positional cloning of the Ttc7 gene required for normal iron homeostasis and mutated in hea and fsn anemia mice. Genomics 85:330–337, 2005.
33. Shultz LD. Hematopoiesis and models of immunodeficiency. Semin Immunol 3:397–408, 1991.
34. Sundberg JP, Beamer WG, Shultz LD, Dunstan RW. Inherited mouse mutations as models of human adnexal, cornification, and papulosquamous dermatoses. J Invest Dermatol 95:62S–63S, 1990.
35. Joliat MJ, Shultz LD. The molecular bases of spontaneous immunological mutations in the mouse and their homologous human diseases. Clin Immunol 101:113–129, 2001.
36. Sonnhammer EL, Eddy SR, Durbin R. Pfam: a comprehensive database of protein domain families based on seed alignments. Proteins 28:405–420, 1997
37. Lamb JR, Tugendreich S. Hieter P. Tetratricopeptide repeat interactions: to TPR or not to TPR? Trends Biochem Sci 20:257–259, 1995.